Journal of Materials Chemistry A

Surface Passivation of Perovskite Thin Films by Phosphonium Halides for Efficient and Stable Solar Cells

Journal:	*Journal of Materials Chemistry A*
Manuscript ID	TA-ART-11-2019-012597.R1
Article Type:	Paper
Date Submitted by the Author:	23-Dec-2019
Complete List of Authors:	He, Qingquan; Florida State University Worku, Michael; Florida State University Xu, Liangjin; Florida State University Zhou, Chenkun; Florida State University, Chemical and Biomedical Engineering; University of Chicago, Chemistry Lteif, Sandrine; Florida State University Schlenoff, Joseph; Florida State University Ma, Biwu; Florida State University, Chemistry and Biochemistry

ARTICLE

Surface Passivation of Perovskite Thin Films by Phosphonium Halides for Efficient and Stable Solar Cells

Received 00th January 20xx,
Accepted 00th January 20xx

DOI: 10.1039/x0xx00000x

Qingquan He,[a] Michael Worku,[b] Liangjin Xu,[a] Chenkun Zhou,[c] Sandrine Lteif,[a] Joe Schlenoff[a] and Biwu Ma*[abc]

Surface passivation of metal halide perovskite thin films has proved to be critical for efficient and stable perovskite solar cells (PSCs), i.e. suppressing charge recombination at the interfaces between perovskite and charge transport layers for high device efficiency and preventing the penetration of degrading agents into the perovskite layer for high device stability. Here, we report the use of a new class of materials, phosphonium halide salts, i.e. triphenyl(9-ethyl-9H-carbazol-3-yl)-phosphonium bromide (TCPBr) and iodide (TCPI), as surface passivation agents for efficient and stable PSCs. Suppressed nonradiative recombination and enhanced interfacial hole extraction, enabled by this facile phosphonium halide passivation, resulted in PSCs with power conversion efficiencies (PCEs) of > 20.1% (~18.5% for pristine $MAPbI_3$ devices). Phosphonium halide passivation also reduced the hysteresis index from 11.2% (pristine device) to 5.4% (TCPBr passivated device). Moreover, the hydrophobic phosphonium halide passivation layers significantly suppressed moisture penetration and ion migration, greatly enhancing the device stability. It was found that unencapsulated solar cells based on TCPBr treated $MAPbI_3$ thin layers retained more than 90% of the initial PCEs after more than 1000 hours storage under ambient conditions. Our work established the potential of phosphonium-based materials for surface passivation of metal halide perovskites, providing a new route towards efficient and stable perovskite optoelectronic devices.

Introduction

Perovskite solar cells (PSCs) have achieved a certified power conversion efficiency (PCE) of 25.2% just one decade after the pioneering work in 2009, thanks to relentless efforts on materials development, processing optimization, and device engineering.[1-8] With impressive PCEs achieved, long-term stability and lead-toxicity are widely considered as two major issues that need to be addressed before commercialization of PSCs. Studies on the degradation of PSCs have suggested a couple of major device efficiency loss pathways. First, perovskite thin films fabricated *via* solution processing are often accompanied by vacancies, substitutions, and interstitial defects, which can serve as charge recombination centers, leading to device efficiency loss.[9-11] Second, the low formation energies of organic-inorganic metal halide perovskites along with ion migrations make them environmentally sensitive, and perovskite thin films could risk degradation on direct exposure to ambient conditions.[12, 13]

To date, many approaches have been developed to prevent the degradation of PSCs, among which surface passivation is perhaps the most successful method employed to improve device efficiency and stability.[14] A variety of materials have been employed to passivate perovskite thin films, including low-dimensional perovskites,[4, 15-20] alkaline halides,[21] polymers,[22-27] inorganic nanocrystals,[28-30] small organic molecules,[31-35], organic halide salts,[5, 10, 12, 36-38], and so on.[19, 39-44] Amine-based organic materials, though perhaps the most investigated, have not been able to fully resolve the stability issues of PSCs. As an important class of organic halide salts, phosphonium halides possess similar electronic characteristics to ammonium halides, which have rarely been investigated for surface passivation of PSCs. Cao and coworkers reported the use of tetraphenylphosphonium chloride (TPPCl) as a processing additive to modulate the morphology and crystallinity of perovskite thin films,[45] which afforded PSCs with a PCE of 13%. Later, they optimized the deposition procedure by treating the PbI_2 film with TPPCl to tune the crystallinity of $MAPbI_3$, which resulted in a PCE of ~18%.[46] Recently, our group demonstrated the use of phosphonium halides, ethane-1,2-diylbis(triphenylphosphonium) bromide and triphenyl(9-ethyl-9H-carbazol-3-yl)-phosphonium bromide (TCPBr) for surface passivation of perovskite nanocrystals,[47, 48] which resulted in significantly enhanced photoluminescence quantum efficiencies and stabilities.

[a] Department of Chemistry and Biochemistry, Florida State University, Tallahassee, FL 32306, USA. E-mail: bma@fsu.edu
[b] Materials Science and Engineering Program, Florida State University, Tallahassee, FL 32306, USA
[c] Department of Chemical and Biomedical Engineering, FAMU-FSU College of Engineering, Tallahassee, FL 32310, USA
†Electronic Supplementary Information (ESI) available. See DOI: 10.1039/x0xx00000x

Motivated by the impressive surface passivation effects of phosphonium halides on perovskite nanocrystals, we extended the concept to perovskite thin films for PSCs. Here we report the use of triphenyl(9-ethyl-9H-carbazol-3-yl)-phosphonium bromide (TCPBr) and iodide (TCPI) for surface passivation of $MAPbI_3$ for efficient and stable planar n-i-p PSCs. Detailed studies show that the incorporation of a phosphonium passivation layer suppressed nonradiative recombination and enhanced the interfacial hole extraction between perovskite and hole transport material (HTM). Consequently, the PCEs of PSCs were improved from ~ 18.5% for pristine $MAPbI_3$ devices to ~ 20.1% for the devices based on TCPBr passivated perovskite thin films. Moreover, the hydrophobic passivation layer resisted moisture and suppressed ion migration, greatly enhanced the device stability with more than 90 % of the initial PCE retained for unencapsulated devices after more than 1000 hours storage under ambient conditions.

Experimental section

Materials

Lead iodide (PbI_2) was bought from TCI. Methylammonium iodide (MAI), *spiro*-OMeTAD, bis(trifluoromethane)sulfonimide lithium salt (Li-TFSI), 4-tert-butylpyridine (t-BP), iodomethane, tin (II) chloride ($SnCl_2$), and thiourea (CH_4N_2S) were purchased from Sigma-Aldrich. FK 209 Co(III) PF_6 salt was bought from Xi'an Polymer Light Technology Corp. All chemicals were used without further purification.

Synthesis of triphenyl(9-ethyl-9H-carbazol-3-yl)-phosphonium bromide (TCPBr) and iodide (TCPI)

The TCPBr halide salts were synthesized according to our previously reported procedures (see Scheme S1 in Supporting Information).[48] Briefly, 3-bromide-9-ethylcarbazole (1 mmol) and $NiBr_2$ (0.1 mmol) were added into 5 mL triphenylphosphine solution (0.2 mM in ethylene glycol) and stirred for 5 h at 170 °C. The solution was cooled down to room temperature and extracted with ethyl ether for several times. For the synthesis of TCPI, TCPBr powder was dissolved in an excess iodomethane solvent and stirred at room temperature for 24 h. The redundant solvent was removed by vacuum to obtain TCPI powder.

Planar n-i-p perovskite solar cells fabrication

The SnO_2 electron transport layer was deposited on clean ITO by spinning the colloidal SnO_2 quantum dots (QDs) solution at 3000 rpm for 30 sec and annealed at 200 °C for 1 h. The synthesis procedure of SnO_2 QDs was modified according to previous report.[49] In brief, $SnCl_2$ (568 mg) and CH_4N_2S (225 mg) were dissolved in an open beaker with deionized water (20 mL) and stirred for 36 h. To make the perovskite solution, MAI and PbI_2 were dissolved in DMF/DMSO (4:1 by vol/vol) with the concentration of 1.3 M. 80 µL of the solution was deposited on an ITO/SnO_2 substrate by two consecutive spin-coating steps of 750 rpm and 4000 rpm for 3 s and 20 s, respectively. At the second step, chlorobenzene (180 uL) was quickly dropped onto the substrate 10 s before the end. Then the substrate was annealed at 100 °C for 10 min to obtain the pristine $MAPbI_3$ perovskite thin films (~ 450 nm thick). The above perovskite solution was diluted to 0.4 mol L^{-1} to prepare thinner $MAPbI_3$ films (~ 100 nm thick). For preparing TCPBr (or TCPI) passivated perovskite thin films, the corresponding phosphonium halide salt was firstly dissolved in isopropanol with the concentration of 0.3, 0.6, and 1.2 mg mL^{-1}. The prepared ITO/SnO_2/$MAPbI_3$ samples were dipped into above solution for 15 s and dried by spinning at 3000 rpm for 30 s. Then the hole transporting layer was deposited by spinning *spiro*-OMeTAD solution at 4000 rpm for 20 s. The solution was prepared by dissolving *spiro*-OMeTAD (50 mg), *t*-BP (18 µL), Li-TFSI solution (10 µL, 517 mg/mL in acetonitrile), and FK 209 (4 µL, 375 mg/mL in acetonitrile) into dried chlorobenzene (0.5 mL). Finally, Au electrode with the thickness of 80 nm was deposited by thermal evaporation under high vacuum (<10^{-6} mbar).

Characterization

X-Ray diffraction (XRD) spectra of the perovskite thin films were measured on a Rigaku SmartLab with Cu Kα radiation. Uv-vis absorption spectra were recorded by a CARY 5000 UV-Vis NIR spectrophotometer (Agilent Technologies). The thickness of perovskite thin films was measured by Dektak 150 profilometer. Scanning electron microscopy (SEM) images were characterized by FEI Nova NanoSEM 400. Atomic force microscope (AFM) topographic was performed on a Bruker Icon scanning probe microscope. The water contact angles of the perovskite thin films were measured by a CAM 200 device (KSV Instruments). The Fourier-transform infrared (FT-IR) spectra were recorded a by PerkinElmer Spectrum 100 FT-IR Spectrometers. Steady-state photoluminescence (PL) and time-resolved PL spectra of perovskite films without and with HTL were measured on Edinburgh FS5 spectrofluorometer. The carrier lifetimes and average lifetime were fitted by biexponential function $y = A_1 \times exp(-x/\tau_1) + A_2 \times exp(-x/\tau_2) + y_0$ and calculated by $\langle\tau\rangle = \Sigma A_i\tau_i^2/\Sigma A_i\tau_i$, respectively. The current density-voltage curves of the devices were measured on the IV5 Solar Cell I-V Measurement System (PV Measurements, Inc.) under the illumination of AM 1.5G in ambient condition with relative humidity of 60%-80%. All the devices were covered by a non-reflective mask with the active area is 0.15 cm^2. The incident photon-to-electron conversion efficiency (IPCE) measurement was carried out by using QEX10 (PV Measurements, Inc.).

Results and Discussion

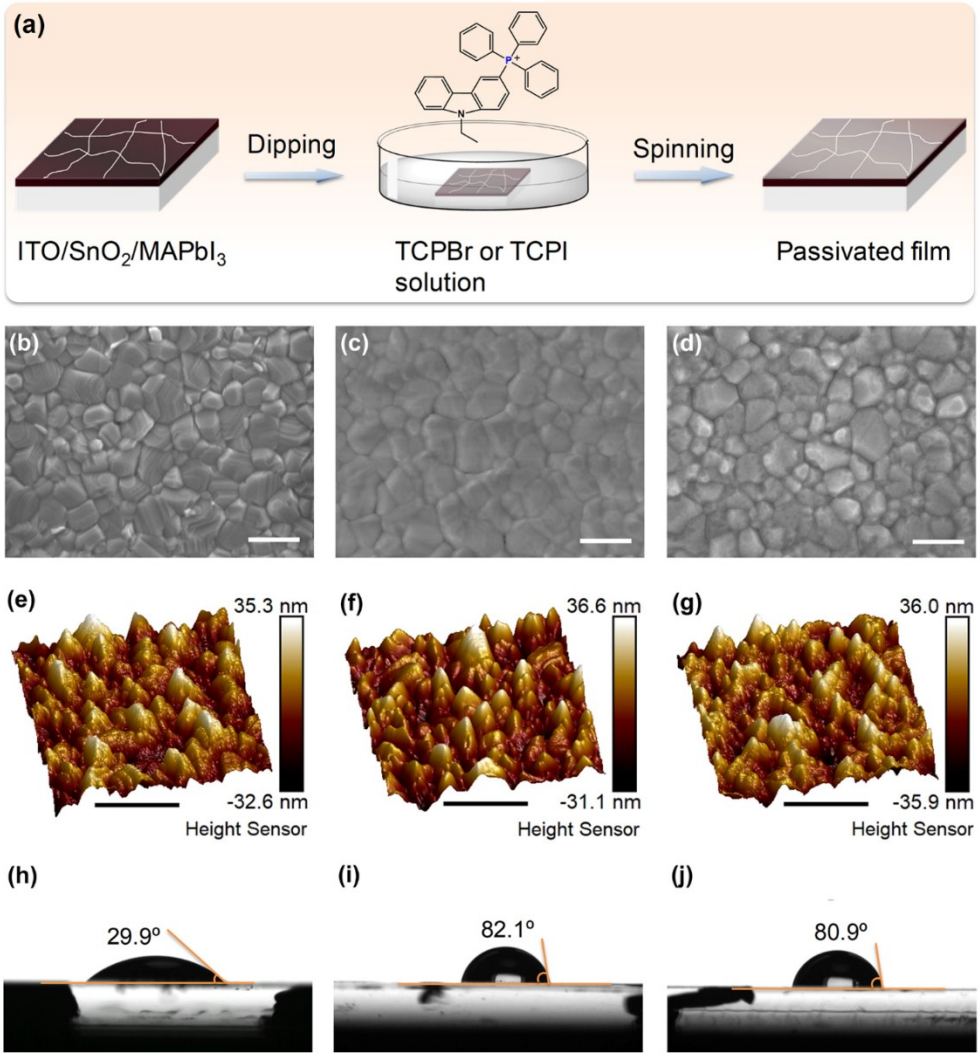

Fig. 1 (a) Schematic illustration of the passivation procedure. SEM and AFM images of (b, e) pristine $MAPbI_3$, (c, f) 0.6 mg mL^{-1} TCPBr, and (d, g) 0.6 mg mL^{-1} TCPI treated perovskites. The scale bar of SEM and AFM images is 500 nm. Contact angle between water and the (h) pristine, (i) TCPBr, and (j) TCPI treated perovskite thin films.

The procedure for fabricating TCPBr (or TCPI) passivated perovskite thin films is shown in Fig. 1a. Briefly, pristine $MAPbI_3$ thin films were deposited on ITO/SnO_2 substrates by a two-step antisolvent method. The ITO/SnO_2/$MAPbI_3$ samples were dipped into a TCPBr (or TCPI) solution (0.6 mg mL^{-1} in isopropanol) for 15 sec, followed by spin drying, to prepare surface passivated thin films. X-ray diffraction (XRD) patterns of pristine perovskite thin films suggest that tetragonal $MAPbI_3$ was obtained (Fig. S1a in Supporting Information). No new peaks were detected after treating with TCPBr or TCPI, indicating that surface passivation did not change the crystal structure of the perovskite thin films. The UV-Vis absorption spectra also remained unchanged after passivation (Fig. S1b), which implies no change to the efficiency of light absorption of the perovskite thin films. To reduce the effect of $MAPbI_3$ substrate to better understand the passivation layer, thinner $MAPbI_3$ films with a thickness of ~ 100 nm were prepared, treated with with TCPBr or TCPI, and characterized, as shown in Fig. S2. Similar to the XRD results in Fig. S1a, no new peaks appeared after surface passivation compared to the pristine $MAPbI_3$ thin films (Fig. S2a). However, increased intensities were observed for the (110) and (220) diffraction peaks, suggesting enhanced crystallinity of surface passivated perovskite thin films.[50] A slight decrease in absorbance was also noted after treating with TCPBr and TCPI (Fig. S2b), which may be attributed to cation exchange between TCP^+ and MA^+ on the surface of $MAPbI_3$ thin films. The largest decrease in absorbance, along with band edge shift to higher energy, was seen in TCPBr treated samples, indicating bromine doping.[51] Fourier transform infrared (FT-IR) spectra of these perovskite thin films show that three peaks locted from 750 to 650 cm^{-1} which belong to phenyl groups were shifted in TCPBr and TCPI treated samples (Fig. S3). A new peak in fingerprint region locted at 1106 cm^{-1} was detected in passivated sample, indicating that TCPBr or TCPI did not physically attach to the surfaces of $MAPbI_3$, but underwent cation exchange with MA^+ in $MAPbI_3$ and/or reacted with PbI_2 to form passivation layer.

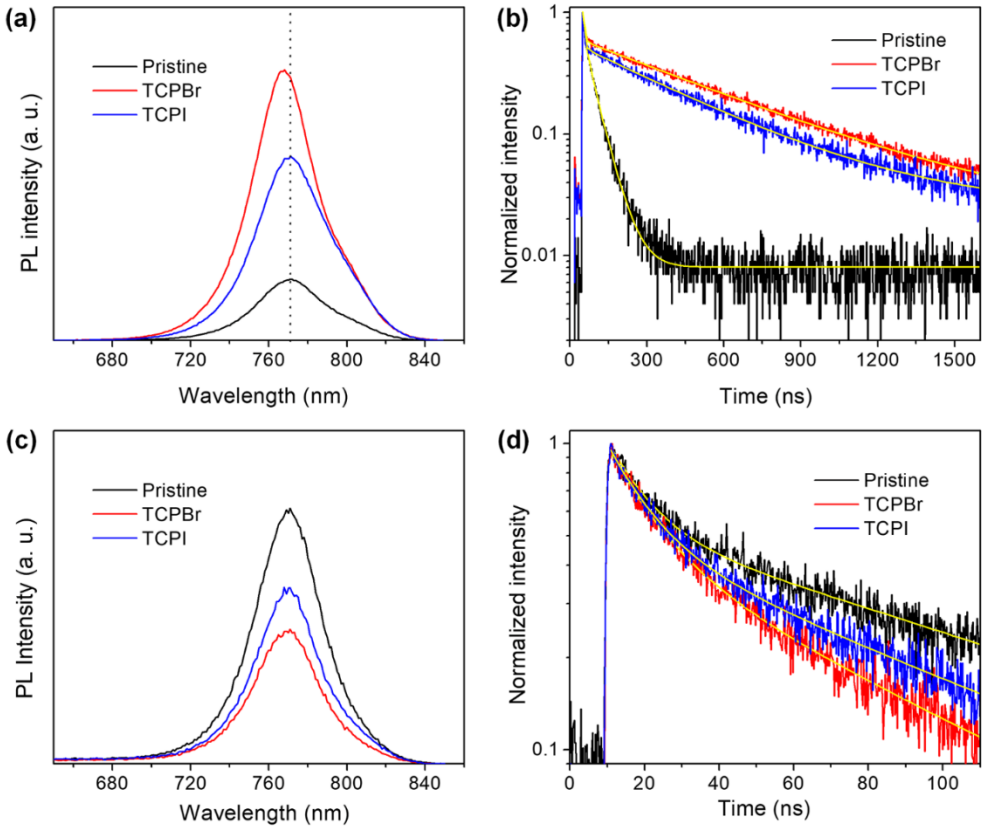

Fig. 2 (a) PL and (b) TRPL spectra of the pristine and TCPBr or TCPI passivated perovskite thin films. (c) PL and (d) TRPL spectra of the perovskite/*spiro*-OMeTAD samples under above treatment conditions.

Scanning electron microscope (SEM) was employed to characterize the morphology of perovskite thin films (Fig. 1b-d). Perovskite crystallites with grain sizes of hundreds of nanometers and clear grain boundaries were observed for the pristine $MAPbI_3$ thin film (Fig. 1b). The grain boundaries blur after treating with TCPBr, and to a lesser extent with TCPI, as shown in Fig. 1c-d. To investigate the effect of surface passivation on the morphologies of perovskite thin films in details, atomic force microscopy (AFM) images were taken (Fig. 1e-g). It can be seen from the 3D AFM images that the surfaces of grains and boundaries of TCPBr treated perokvsite thin film are smoother than those of pristine and TCPI passivated samples. These results are consistent with SEM characterizations and confirm the surface passivation effect of phosphonium halide salts. The hydrophobicity of surface passivated perovskite thin films was investigated by contact angle measurements. Fig. 1h-j show the contact angles increased significantly from 29.9° for pristine $MAPbI_3$ thin film to 82.1° and 80.9° for TCPBr and TCPI treated samples, respectively. The difference in the passivation effects of TCPBr and TCPI may be attributed to bromide doping imparted by TCPBr.

To investigate the influence of surface passivation on photogenerated charge carriers, steady-state photoluminescence (PL) spectra of perovskite thin films were recorded, as shown in Fig. 2a. The PL peak intensity was greatly enhanced after treating with TCPBr compared to the pristine $MAPbI_3$, indicating nonradiative recombination rate was significantly reduced. The PL peak of TCPBr treated sample is clearly higher than that of the TCPI treated one, suggesting more efficient surface passivation after bromide doping. Moreover, a small blue shift of the PL peak for the TCPBr treated sample supported bromide doping, implying a lower trap density near the band-edge of the passivated perovskite thin film (Fig. S4a),[38, 50] which is consistent with the UV-Vis absorption spectrum discussed above. Additionally, the same measurement was performed on the back side of the perovskite thin films (Fig. S4b). Almost identical PL spectra for all the samples were collected after normalizing, indicating that the passivation layer was generated only at the surface of $MAPbI_3$. The corresponding PL decay lifetimes of the passivated perovskite thin films were measured by time-resolved PL (TRPL) and fitted with a biexponential decay model (Fig. 2b, Table S1 in Supporting Information). The relatively fast decay component (τ_1) was assigned to charge carrier trapping induced by trap states at grain boundaries and/or surfaces (non-radiative recombination) while the slower decay component (τ_2) was associated with free carrier recombination (radiative recombination).[28, 52, 53] The proportion of τ_1 (A_1) decreases from 30.2% for pristine $MAPbI_3$ to 5.4% and 8.9% for TCPBr and TCPI passivated samples, respectively, while the corresponding τ_2 significantly elongates from 79.4 ns to 531.1 ns and 422.2 ns. Thus, passivation not only greatly

decreased the defect density, thereby suppressing the nonradiative recombination, but also increased the crystallinity of perovskite thin films, improving the radiative recombination as discussed above.[50, 54, 55]

suggests that the TCPBr passivated perovskite thin film (13.0 ns) inject holes into HTM faster than the pristine (18.8 ns) and TCPI (15.9 ns) treated samples, implying an improvement of the hole extraction process at the interface of perovskite thin film and HTL.[57]

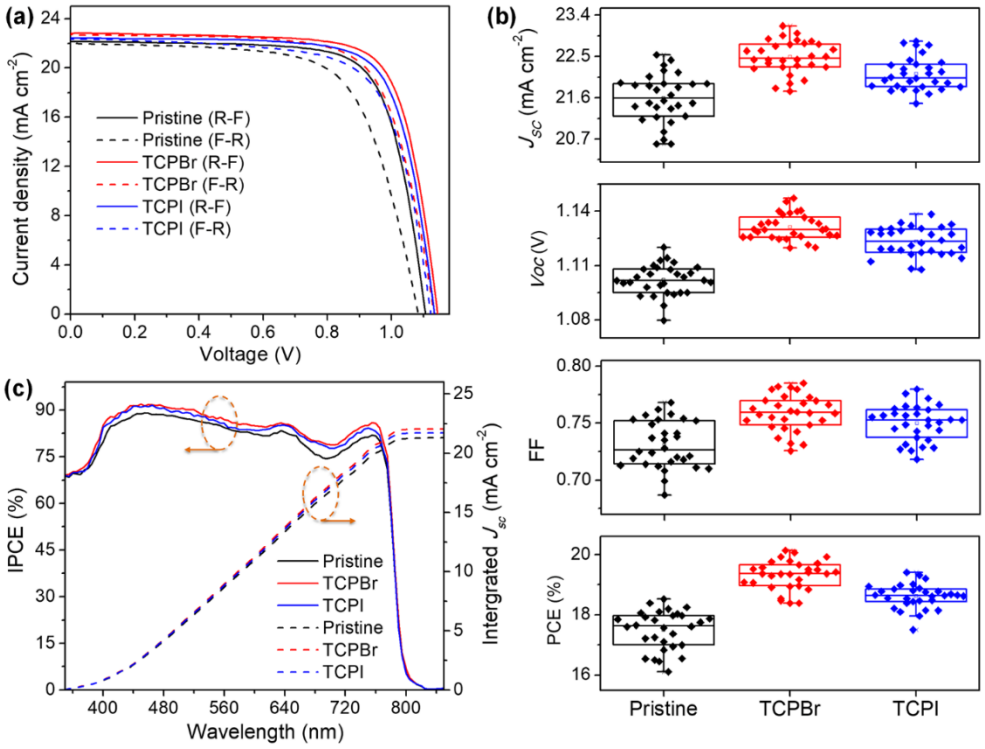

Fig. 3 (a) Current density-voltage (*J-V*) characteristics in reverse and forward scans of PSCs based on perovskite thin films treated with different halide salts. (b) The statistical distribution of J_{SC}, V_{OC}, FF, and PCE for the devices. Statistics from 30 devices for each sample. (c) IPCE and the corresponding integrated J_{SC} curves of PSCs.

Charge transfer dynamics between the perovskite and HTM were further investigated as shown in Fig. 2c. In the presence of *spiro*-OMeTAD, the PL of TCPI passivated perovskite thin film was strongly quenched as compared to that of the pristine film, indicating that the surface passivation accelerates carrier extraction from perovskite to hole transport layer (HTL).[5, 50, 56] Furthermore, the lowest PL peak intensity of the TCPBr treated sample suggested the fastest charge carrier extraction. TRPL measurements were performed and fitted with a biexponential decay curve (Fig. 2d, Table S2). The result

Encouraged by the high quality of the passivated perovskite thin films and efficient charge extraction at the perovskite/HTM interfaces, planar n-i-p PSCs were fabricated and tested as shown in Fig. 3 and Fig. S5. By tuning the amount of TCPBr and TCPI in the treatment solutions the optimal concentration was found to be 0.6 mg mL^{-1} (Fig. S6, Table S3-S4). Fig. 3a displays the *J-V* characteristics in reverse and forward scans of the best performing PSCs. The corresponding photovoltaic parameters are summarized in Table S5. The

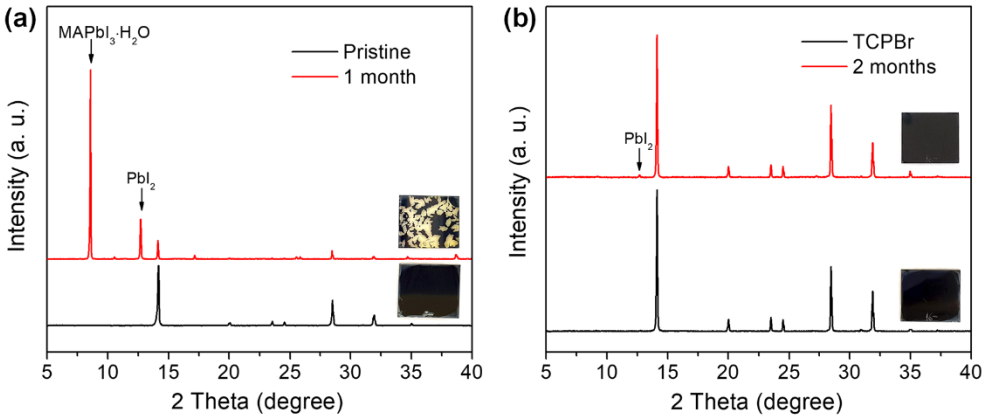

Fig. 4 XRD patterns of (a) pristine $MAPbI_3$ and (b) TCPBr treated perovskite thin films before and after exposure to ambient conditions with 60-80% RH at room temperature. The insets are the corresponding photographic images of perovskite thin films.

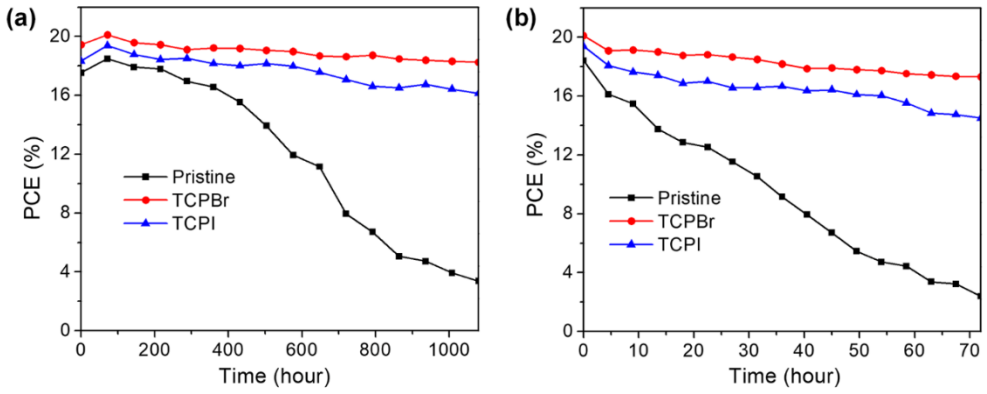

Fig. 5 PCE evolution of the unencapsulated PSCs based on different perovskite thin films (a) stored in dark and (b) illuminated under AM 1.5G measured in ambient conditions (~ 40 ^{o}C, 60-80% RH).

pristine $MAPbI_3$ device had a PCE of 18.52% with a J_{SC} of 22.15 mA cm^{-2}, a V_{oc} of 1.11 V, and an FF of 0.75. The device based on TCPBr treated perovskite thin film exhibited an improved J_{SC} of 22.63 mA cm^{-2}, a V_{OC} of 1.14 V, an FF of 0.78, and a PCE of 20.13%. The TCPBr treated device performed slightly better than the TCPI treated one, which displayed a J_{SC} of 22.42 mA cm^{-2}, a V_{OC} of 1.13 V, an FF of 0.77, and a PCE of 19.41%. The enhanced PCEs of passivated devices are attributed to the passivation layers on the surface of $MAPbI_3$ thin films, which deactivate surface traps thereby reducing nonradiative recombination and accelerating hole tranfer across the perovskite/HTM interface.

The hysteresis behavior (H = ($PCE_{reverse}$ - $PCE_{forward}$)/$PCE_{reverse}$) of the PSCs was also improved after surface passivation by phosphonium halides (Fig. 3a). The device based on TCPBr passivated perovskite thin film achieved the lowest hysteresis index (5.4%), compared to those of the pristine (11.2%) and TCPI treated (5.6%) samples. The improvement of hysteresis may be ascribed to the passivation layer which not only deactivated the surface traps of $MAPbI_3$, thereby reducing the nonradiative recombination, but also suppressed the migration of iodide ions and inhibited ion accumulation at the interface between the perovskite and HTM.[15, 58] The higher PCE and lower hysteresis index of TCPBr treated devices than those of TCPI treated ones further implies more efficient passivation of TCPBr as discussed above. To evaluate the reproducibility of PSCs , 30 devices were fabricated for each case (Fig. 3b and Table S6). The results indicate that the trends of changes for all average photovoltaic characteristics are well matched with the best performing devices discussed in Fig. 3a, comfirming the reliability of our testing results. IPCE measurements of the devices were performed with results shown in Fig. 3c. The corresponding J_{SC} was integrated revealing that the device containing TCPBr passivated perovskite layer can reach to 22.04 mA cm^{-2}. This value is higher than the pristine $MAPbI_3$ (21.29 mA cm^{-2}) and TCPI treated device (21.77 mA cm^{-2}), which is in agreement with the corresponding J_{SC} value derived from the J-V measurement (~ 3%), further confirming the passivation effect of the TCPBr and TCPI. Additionally, another control experiments based on phenethylammonium iodide (PEAI) passivation agent were performed under the same conditions to show the advantages of phosphonium halides passivation agents (see details in Figure S7-S9 and Table S7).The results indicated that the treatment of PEAI could reduce the nonradiative recombination of perovskite thin films, thereby improved the efficiencies of PSCs from ~ 18.5% for pristine devices to ~ 18.8% for PEAI treated devices. However, the passivation effectiveness of PEAI is still lower than those of TCPBr and TCPI.

To investigate the stabilities of pristine and surface passivated $MAPbI_3$ thin films, XRD was used to characterize the samples stored in ambient conditions with a relative humidity (RH) of 60-80% for one or two months. As shown in Fig. 4, diffraction peaks belonging to $MAPbI_3{\cdot}H_2O$ and PbI_2 appeared for the pristine $MAPbI_3$ thin film after one month, indicating hydration and decomposition of the thin film (Fig. 4a).[59] In comparison, only a small diffraction peak attributable to PbI_2 can be observed in the XRD patterns of TCPBr and TCPI treated $MAPbI_3$ thin films after ambient exposure for two months (Fig. 4b and Fig. S10). The significant enhancement of stability by phosphonium halide passivation could be attributed to the hydrophobic nature of TCP^+ with ethylene group and bulkier structure prohibiting moisture permeation, as confirmed by the contact angle measurements in Fig. 1i and 1j.

The storage and illumination stability of unencapsulated PSCs were further investigated under ambient conditions (Fig. 5). Fig. 5a displays the PCE evolution of devices after more than 1000 hours of storage in ambient conditions (room temperature, 60-80 % RH). The device based on TCPBr treated perovskite thin film retained 90.7% of its initial PCE, which is higher than that of TCPI (83.2%). In contrast, the pristine $MAPbI_3$ device showed significant reductions in performance and only 18.2% of its initial PCE remained. For the illumination stability, the device fabricated with pristine $MAPbI_3$ also showed a fast decline of PCE with nearly 90% performance loss after exposure to AM 1.5G for 72 hours (~ 40 ^{o}C, 60-80% RH) as shown in Fig. 5b. In comparison, the devices passivated by TCPBr and TCPI retained 86.1% and 74.9% of their initial PCE, respectively. These results indicate the stability of PSCs can be

greatly enhanced after treating with TCPBr and TCPI. The introduction of hydrophobic phosphonium-based passivation layers on the surface of $MAPbI_3$ thin films not only served as water-deterring "cover" to resist the moisture attack, but also suppressed ion migration during device operation, thus greatly enhancing the device stability.

Conclusions

In conclusion, we have demonstrated surface passivation of perovskite thin films by phosphonium-based organic halide salts to achieve efficient and stable perovskite solar cells. It was found that the introduction of a passivation layer on the surface of $MAPbI_3$ thin film deactivated the surface traps thereby reducing nonradiative recombination and accelerated hole tranfer across the perovskite/HTM interface. Moreover, the hydrophobic phosphonium-based passivation layer could serve as water-deterring "cover" to resist moisture, as well as suppress ion migration during the device operation, greatly improving the hysteresis behavior and stability of devices. This facile and effective surface passivation strategy based on phosphonium organic halide salts provides a new means to enhance the photovoltaic performances and environmental stability of PSCs, which could also be useful for other optoelectronic devices based on metal halide perovskites.

Conflicts of interest

There are no conflicts to declare.

Acknowledgements

The authors acknowledge the supports from the National Science Foundation (DMR-1709116), the Air Force Office of Scientific Research (AFOSR) (17RT0906), and the FSU Office of Research.

References

1. A. Kojima, K. Teshima, Y. Shirai and T. Miyasaka, *J. Am. Chem. Soc.*, 2009, **131**, 6050.
2. N. J. Jeon, J. H. Noh, W. S. Yang, Y. C. Kim, S. Ryu, J. Seo and S. I. Seok, *Nature*, 2015, **517**, 476.
3. N. Arora, M. I. Dar, A. Hinderhofer, N. Pellet, F. Schreiber, S. M. Zakeeruddin and M. Gratzel, *Science*, 2017, **358**, 768.
4. E. H. Jung, N. J. Jeon, E. Y. Park, C. S. Moon, T. J. Shin, T.-Y. Yang, J. H. Noh and J. Seo, *Nature*, 2019, **567**, 511.
5. Q. Jiang, Y. Zhao, X. Zhang, X. Yang, Y. Chen, Z. Chu, Q. Ye, X. Li, Z. Yin and J. You, *Nat. Photonics*, 2019, **13**, 460.
6. A. F. Castro-Mendez, J. Hidalgo and J. P. Correa-Baena, *Adv. Energy Mater.*, 2019, **9**, 1901489.
7. J.-H. Im, C.-R. Lee, J.-W. Lee, S.-W. Park and N.-G. Park, *Nanoscale*, 2011, **3**, 4088.
8. H.-S. Kim, C.-R. Lee, J.-H. Im, K.-B. Lee, T. Moehl, A. Marchioro, S.-J. Moon, R. Humphry-Baker, J.-H. Yum, J. E. Moser, M. Graetzel and N.-G. Park, *Sci. Rep.*, 2012, **2**, 591.
9. S. Fu, X. Li, L. Wan, Y. Wu, W. Zhang, Y. Wang, Q. Bao and J. Fang, *Adv. Energy Mater.*, 2019, **9**, 1901852.
10. X. P. Zheng, B. Chen, J. Dai, Y. J. Fang, Y. Bai, Y. Z. Lin, H. T. Wei, X. C. Zeng and J. S. Huang, *Nat. Energy*, 2017, **2**, 17102.
11. C. Zhou, H. Lin, Q. He, L. Xu, M. Worku, M. Chaaban, S. Lee, X. Shi, M.-H. Du and B. Ma, *Materials Science and Engineering: R: Reports*, 2019, **137**, 38.
12. H. Dong, J. Xi, L. Zuo, J. Li, Y. Yang, D. Wang, Y. Yu, L. Ma, C. Ran, W. Gao, B. Jiao, J. Xu, T. Lei, F. Wei, F. Yuan, L. Zhang, Y. Shi, X. Hou and Z. Wu, *Adv. Funct. Mater.*, 2019, **29**, 1808119.
13. E. B. Bi, H. Chen, F. X. Xie, Y. Z. Wu, W. Chen, Y. J. Su, A. Islam, M. Gratzel, X. D. Yang and L. Y. Han, *Nat. Commun.*, 2017, **8**, 15330.
14. B. Chen, P. N. Rudd, S. Yang, Y. B. Yuan and J. S. Huang, *Chem. Soc. Rev.*, 2019, **48**, 3842.
15. L. Gao, I. Spanopoulos, W. Ke, S. Huang, I. Hadar, L. Chen, X. Li, G. Yang and M. G. Kanatzidis, *ACS Energy Lett.*, 2019, **4**, 1763.
16. Q. Zhou, L. Liang, J. Hu, B. Cao, L. Yang, T. Wu, X. Li, B. Zhang and P. Gao, *Adv. Energy Mater.*, 2019, **9**, 1802595.
17. D. Lin, T. Zhang, J. Wang, M. Long, F. Xie, J. Chen, B. Wu, T. Shi, K. Yan, W. Xie, P. Liu and J. Xu, *Nano Energy*, 2019, **59**, 619.
18. B. Liu, M. Long, M. Cai, L. Ding and J. Yang, *Nano Energy*, 2019, **59**, 715.
19. Y. Bai, S. Xiao, C. Hu, T. Zhang, X. Y. Meng, H. Lin, Y. L. Yang and S. H. Yang, *Adv. Energy Mater.*, 2017, **7**, 1701038.
20. M. Z. Long, T. K. Zhang, D. C. Chen, M. C. Qin, Z. F. Chen, L. Gong, X. H. Lu, F. Y. Xie, W. G. Xie, J. Chen and J. B. Xu, *ACS Energy Lett.*, 2019, **4**, 1025.
21. X. Liu, Y. F. Zhang, L. Shi, Z. H. Liu, J. L. Huang, J. S. Yun, Y. Y. Zeng, A. B. Pu, K. W. Sun, Z. Hameiri, J. A. Stride, J. Seidel, M. A. Green and X. J. Hao, *Adv. Energy Mater.*, 2018, **8**, 1800138.
22. X. R. Wen, J. M. Wu, M. D. Ye, D. Gao and C. J. Lin, *Chem. Commun.*, 2016, **52**, 11355.
23. M. H. Li, X. Q. Yan, Z. Kang, Y. H. Huang, Y. Li, R. X. Zhang and Y. Zhang, *ACS Appl. Mater. Interfaces*, 2018, **10**, 18787.
24. L. B. Huang, P. Y. Su, J. M. Liu, J. F. Huang, Y. F. Chen, S. Qin, J. Guo, Y. W. Xu and C. Y. Su, *J. Power Sources*, 2018, **378**, 483.
25. F. L. Cai, J. L. Cai, L. Y. Yang, W. Li, R. S. Gurney, H. N. Yi, A. Iraqi, D. Liu and T. Wang, *Nano Energy*, 2018, **45**, 28.
26. D. J. Fairfield, H. Sai, A. Narayanan, J. V. Passarelli, M. Chen, J. Palasz, L. C. Palmer, M. R. Wasielewski and S. I. Stupp, *J. Mater. Chem. A*, 2019, **7**, 1687.
27. W. Chen, Y. F. Wang, G. T. Pang, C. W. Koh, A. B. Djurisic, Y. H. Wu, B. Tu, F. Z. Liu, R. Chen, H. Y. Woo, X. G. Guo and Z. B. He, *Adv. Funct. Mater.*, 2019, **29**, 1808855.
28. W. Zhou, S. Chen, Y. Zhao, Q. Li, Y. Zhao, R. Fu, D. Yu, P. Gao and Q. Zhao, *Adv. Funct. Mater.*, 2019, **29**, 1809180.
29. Y. F. Dou, D. Wang, G. D. Li, Y. S. Liao, W. H. Sun, J. H. Wu and Z. Lan, *ACS Appl. Mater. Interfaces*, 2019, **11**, 32159.
30. C. Liu, M. M. Hu, X. Y. Zhou, J. C. Wu, L. Z. Zhang, W. G. Kong, X. N. Li, X. Z. Zhao, S. Y. Dai, B. M. Xu and C. Cheng, *Npg Asia Materials*, 2018, **10**, 552.
31. M. Abdi-Jalebi, M. I. Dar, S. P. Senanayak, A. Sadhanala, Z. Andaji-Garmaroudi, L. M. Pazos-Outon, J. M. Richter, A. J. Pearson, H. Sirringhaus, M. Gratzel and R. H. Friend, *Sci. Adv.*, 2019, **5**, eaav2012.
32. W. Q. Wu, Z. B. Yang, P. N. Rudd, Y. C. Shao, X. Z. Dai, H. T.

Wei, J. J. Zhao, Y. J. Fang, Q. Wang, Y. Liu, Y. H. Deng, X. Xiao, Y. X. Feng and J. S. Huang, *Sci. Adv.*, 2019, **5**, eaav8925.
33. H. Zhang, Y. Wu, C. Shen, E. Li, C. Yan, W. Zhang, H. Tian, L. Han and W.-H. Zhu, *Adv. Energy Mater.*, 2019, **9**, 1803573.
34. F. Tan, H. Tan, M. I. Saidaminov, M. Wei, M. Liu, A. Mei, P. Li, B. Zhang, C.-S. Tan, X. Gong, Y. Zhao, A. R. Kirmani, Z. Huang, J. Z. Fan, R. Quintero-Bermudez, J. Kim, Y. Zhao, O. Voznyy, Y. Gao, F. Zhang, L. J. Richter, Z.-H. Lu, W. Zhang and E. H. Sargent, *Adv. Mater.*, 2019, **31**, 1807435.
35. P. F. Guo, Q. Ye, X. K. Yang, J. Zhang, F. Xu, D. Shchukin, B. Q. Wei and H. Q. Wang, *J. Mater. Chem. A*, 2019, **7**, 2497.
36. Y. Z. Zhang, M. J. Rong, X. Y. Yan, X. L. Wang, Y. L. Chen, X. Y. Li and R. M. Zhu, *Langmuir*, 2018, **34**, 9507.
37. X. N. Bu, R. J. E. Westbrook, L. Lanzetta, D. Ding, T. Chotchuangchutchaval, N. Aristidou and S. A. Haque, *Sol. RRL*, 2019, **3**, 1800282.
38. Y. Wang, T. Y. Zhang, M. Kan and Y. X. Zhao, *J. Am. Chem. Soc.*, 2018, **140**, 12345.
39. H. Li, L. M. Tao, F. H. Huang, Q. Sun, X. J. Zhao, J. B. Han, Y. Shen and M. K. Wang, *ACS Appl. Mater. Interfaces*, 2017, **9**, 38967.
40. X. X. Feng, R. H. Chen, Z. A. Nan, X. D. Lv, R. Q. Meng, J. Cao and Y. Tang, *Adv. Sci.*, 2019, **6**, 1802040.
41. F. Qian, S. Yuan, Y. Cai, Y. Han, H. Zhao, J. Sun, Z. Liu and S. Liu, *Sol. RRL*, 2019, **3**, 1900072.
42. Y. Bai, Y. Lin, L. Ren, X. Shi, E. Strounina, Y. Deng, Q. Wang, Y. Fang, X. Zheng, Y. Lin, Z.-G. Chen, Y. Du, L. Wang and J. Huang, *ACS Energy Lett.*, 2019, **4**, 1231.
43. S. Yang, S. S. Chen, E. Mosconi, Y. J. Fang, X. Xiao, C. C. Wang, Y. Zhou, Z. H. Yu, J. J. Zhao, Y. L. Gao, F. De Angelis and J. S. Huang, *Science*, 2019, **365**, 473.
44. W. S. Yang, B. W. Park, E. H. Jung, N. J. Jeon, Y. C. Kim, D. U. Lee, S. S. Shin, J. Seo, E. K. Kim, J. H. Noh and S. I. Seok, *Science*, 2017, **356**, 1376.
45. C. Sun, Q. F. Xue, Z. C. Hu, Z. M. Chen, F. Huang, H. L. Yip and Y. Cao, *Small*, 2015, **11**, 3344.
46. J. Qi, X. Yao, W. Z. Xu, X. Wu, X. F. Jiang, X. Gong and Y. Cao, *ACS Omega*, 2018, **3**, 7069.
47. L.-J. Xu, M. Worku, H. Lin, Z. Xu, Q. He, C. Zhou, H. Zhang, Y. Xin, S. Lteif, J. Xue and B. Ma, *J. Phys. Chem. Lett.*, 2019, **10**, 5923.
48. L.-J. Xu, M. Worku, Q. He, H. Lin, C. Zhou, B. Chen, X. Lin, Y. Xin and B. Ma, *J. Phys. Chem. Lett.*, 2019, **10**, 5836.
49. G. Yang, C. Chen, F. Yao, Z. Chen, Q. Zhang, X. Zheng, J. Ma, H. Lei, P. Qin, L. Xiong, W. Ke, G. Li, Y. Yan and G. Fang, *Adv. Mater.*, 2018, **30**, 1706023.
50. S. Yuan, F. Qian, S. Yang, Y. Cai, Q. Wang, J. Sun, Z. Liu and S. Liu, *Adv. Funct. Mater.*, 2019, **29**, 1807850.
51. A. H. Proppe, M. Wei, B. Chen, R. Quintero-Bermudez, S. O. Kelley and E. H. Sargent, *J. Am. Chem. Soc.*, 2019, **141**, 14180.
52. J. W. Lee, Z. H. Dai, T. H. Han, C. Choi, S. Y. Chang, S. J. Lee, N. De Marco, H. X. Zhao, P. Y. Sun, Y. Huang and Y. Yang, *Nat. Commun.*, 2018, **9**, 3021.
53. S. G. Kim, J. Chen, J. Y. Seo, D. H. Kang and N. G. Park, *ACS Appl. Mater. Interfaces*, 2018, **10**, 25372.
54. Y. Liu, S. Akin, L. Pan, R. Uchida, N. Arora, J. V. Milić, A. Hinderhofer, F. Schreiber, A. R. Uhl, S. M. Zakeeruddin, A. Hagfeldt, M. I. Dar and M. Grätzel, *Sci. Adv.*, 2019, **5**, eaaw2543.
55. D. Lee, J. S. Yun, J. Kim, A. M. Soufiani, S. Chen, Y. Cho, X. F. Deng, J. Seidel, S. Lim, S. J. Huang and A. W. Y. Ho-Baillie, *ACS Energy Lett.*, 2018, **3**, 647.
56. K. T. Cho, S. Paek, G. Grancini, C. Roldan-Carmona, P. Gao, Y. H. Lee and M. K. Nazeeruddin, *Energy Environ. Sci.*, 2017, **10**, 621.
57. Y. T. Chen, X. W. Xu, N. Cai, S. N. Qian, R. X. Luo, Y. P. Huo and S. W. Tsang, *Adv. Energy Mater.*, 2019, **9**, 1901268.
58. Y. Y. Cho, A. M. Soufiani, J. S. Yun, J. C. Kim, D. S. Lee, J. Seidel, X. F. Deng, M. A. Green, S. J. Huang and A. W. Y. Ho-Baillie, *Adv. Energy Mater.*, 2018, **8**, 1703392.
59. M. G. Ju, M. Chen, Y. Y. Zhou, J. Dai, L. Ma, N. P. Padture and X. C. Zeng, *Joule*, 2018, **2**, 1231.

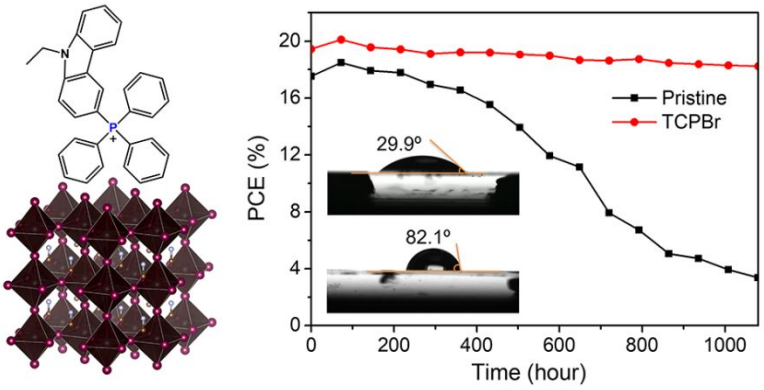

A new class of materials, phosphonium halide salts, are used as surface passivation agents for efficient and stable PSCs.